DOI: 10.13009/EUCASS2017-619

On the Structure of Large Scale Separations in Hypersonic Flows

Sudhir L. Gai, Amna Khraibut, and Gaetano M. D. Currao

School of Engineering and Technology, University of New South Wales
Northcott Drive, Canberra, Australia

Abstract

Structure of large hypersonic boundary layer separation and reattachment is considered within the framework of asymptotic theory of Nieland and Stewartson. It is shown that the separation bubble length and second minimum in shear stress are uniquely related to the perturbation strength expressed in terms of a scaled angle α and that this is independent of the mode provoking separation.

1. Introduction

In recent years, in several investigations of supersonic and hypersonic shock wave/boundary layer interactions (SWBLI), involving large separated regions, numerical studies have shown multiple vortex structures/eddies embedded in the main separation bubble (Neiland et al. [1]; Shvedchenko [2]; Smith and Khorrami [3]; Korolev et al. [4]). The Effects of wall temperature and Reynolds number on the development of these multiple eddies has also been discussed by Neiland et al. [1]and Shvedchenko [2]. The critical parameter governing the origin and existence of these eddies seems to be the angle $\alpha = O(Re^{1/4})$ which represents the strength of perturbation to the boundary layer such as shock wave provoking separation at a compression corner or a shock wave from a wedge incident on a boundary layer growing over a surface such as a flat plate beneath the wedge. It must be emphasized that the existence of these eddies is based mainly on numerical simulations of two-dimensional flows involving large separated regions created by large pressure perturbations such as compression ramp angles. So far, there seems to have been no experimental confirmation of this phenomenon except in very few specific instances.

In the present paper, we discuss the presence of such eddies in large separated regions in moderate to low enthalpy hypersonic flows under different scenarios – (i) a compression corner; (ii) a leading edge separation; and (iii) an incident shock on a boundary layer over a flat plate.

2. Some Theoretical Considerations

A separation bubble is said to be small when the length of the bubble is $O(lRe^{-3/8})$ or less and both separation and reattachment are contained within it. Here, l is the characteristic length such as the distance from the leading edge to the compression corner or the point of incidence of an incident shock on a boundary layer over a flat plate. Re is a characteristic Reynolds number based on l and freestream/boundary layer edge conditions. In subsequent discussion, we sometimes use the triple-deck controlling parameter $\varepsilon = Re^{-1/8}$ so that $O(lRe^{-3/8})$ becomes $O(l\varepsilon^3)$. If the bubble length is greater or equal to $O(l)$, separation is said to be large (Burggraf [5]; Korolev et al. [4]). Another characteristic of large separation bubble is that it consists of three distinct but contiguous regions – an initial rise, up to separation, with length of $O(l\varepsilon^3)$, the Chapman free-interaction region, a large plateau region of constant pressure $O(l)$, which is followed by the reattachment region of $O(l\varepsilon^4)$ in extent that is largely an inviscid process (see Daniels [6]). **Fig. 1** shows a schematic of such a flow structure.

DOI: 10.13009/EUCASS2017-619

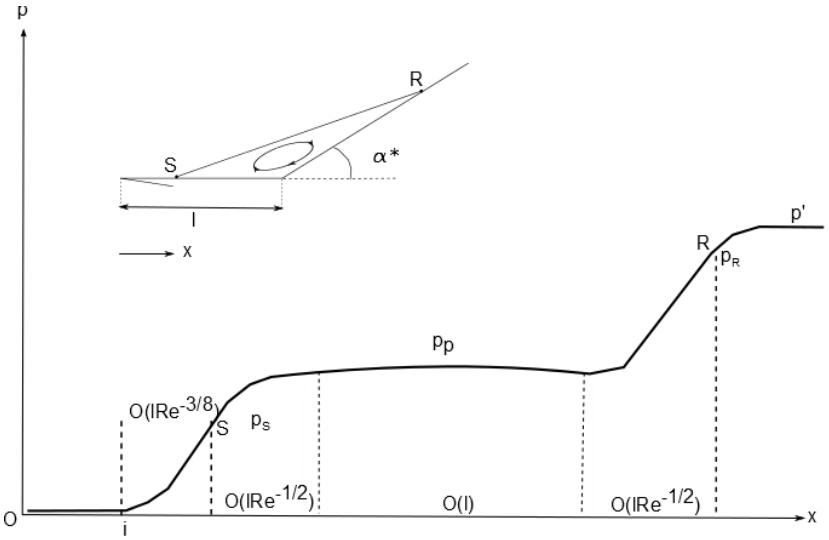

Figure 1: Pressure Distribution in a large separation region.

Referring to **Fig. 1**, the point wherein separation just appears (*S*) – the so-called incipient separation, the scaled angle α has a value $\alpha_i = 1.57$ (Rizzetta et al. [7]; Smith and Khorrami [3]) and can be completely described in terms of triple-deck theory. It is also consistent with Chapman's free-interaction theory (Chapman et al. [8]). Burggraf [5], Korolev et al. [4], Neiland et al. [1] have argued that even large separation regions are amenable to analysis in terms of triple-deck theory.

We will now consider each of the regions depicted in **Fig. 1** in turn.

2.1 Separation Region

Stewartson and Williams [9] have described the flow near separation in planar flow in terms of four regions as shown in **Fig. 2**. Region I consists of a forward moving inviscid supersonic/hypersonic flow. Region III delineates a largely inviscid slow moving reverse flow. The boundary layer which separates at x_s forms the mixing layer region II, while a sub-boundary layer (region IV) that forms beneath region III and flows in the reverse direction joins smoothly with region II at x_s, so that the dividing streamline separates the forward and reverse flows. These regions are consistent with the triple-deck assumptions. The symbol ε in the figure denotes triple-deck scaling parameter $Re^{-1/8}$, where $Re = u_\infty x_s/\nu_\infty$. The angle θ_s which the dividing streamline makes with the surface can be determined through the Oswatitsch formula relating the streamwise shear stress and pressure gradients at the point of separation.

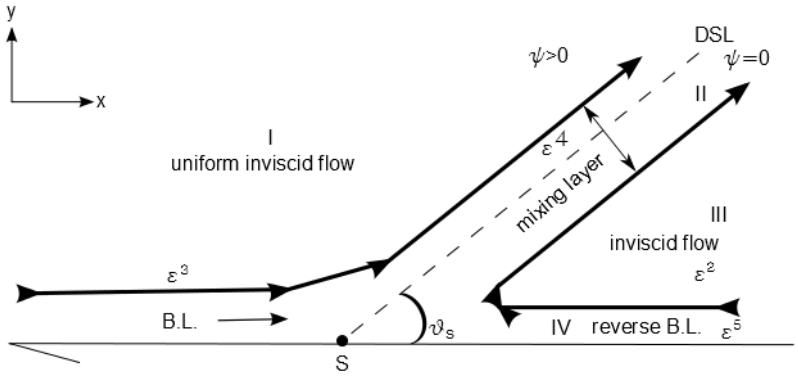

Figure 2: Flow at separation (after Stewartson and Williams [9]).

DOI: 10.13009/EUCASS2017-619

2.2 Reattachment Region

The reattachment region is simply the reverse of separation so that the basic flow features will be similar. Daniels [6] has shown that the triple-deck structure is equally valid in the reattachment region (**Fig. 3**). As in the case of separation, the flow in the immediate vicinity of reattachment can be considered independent of the overall flow configuration. Daniels treats the reattachment process using the triple-deck theory making a point that the phenomenon, although largely inviscid, is still dominated by viscous processes near the wall so that the reattachment pressure is different from the recompression shock pressure *p'* which is the consequence of an inviscid process. This was also pointed out by Chapman et al. [8] while proposing their isentropic recompression theory, which ignores the role of viscosity in the reattachment process. This is illustrated in **Fig. 1** wherein p_r is different from *p'*, showing that the actual recompression process as a whole is non-isentropic. The description of the reattachment process in the context of triple-deck theory has also been given by Gittler and Kluwick [10] and Korolev et al. [4] wherein the rise in pressure due to recompression process is shown to vary as $\Delta p \sim \alpha$.

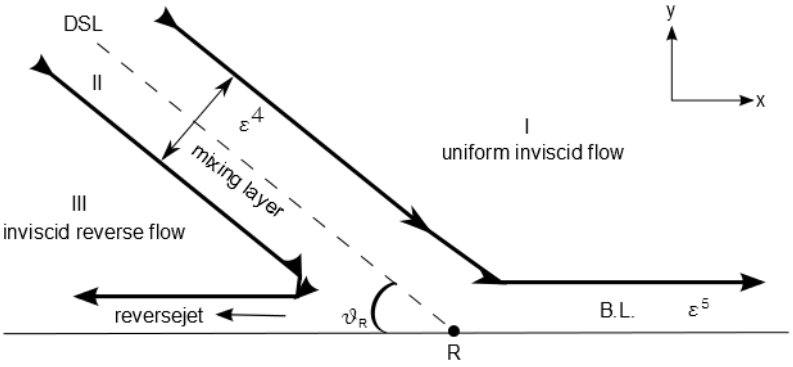

Figure 3: Reattachment region.

These viscous effects are accentuated in hypersonic SBLIs. Typically, in a high Mach number SBLI, the boundary layer in the reattachment region becomes very thin and confluence of separation and reattachment shocks (and sometimes the leading edge shock) occurs very close to the surface. This generates strong coalescence of compression waves at the triple-point from whence a slip stream and centred expansion waves originate and reflect from the surface. The overall effect is then the so called 'necking' with a pressure over-shoot followed by a rapid decrease before the pressure attains a constant value *p'*. **Fig. 4** shows such a state of affairs. The shock/shock/expansion interaction at the triple-point *P* shown in the inset gives rise to what is known as the Edney Type VI interaction (Edney [11]).

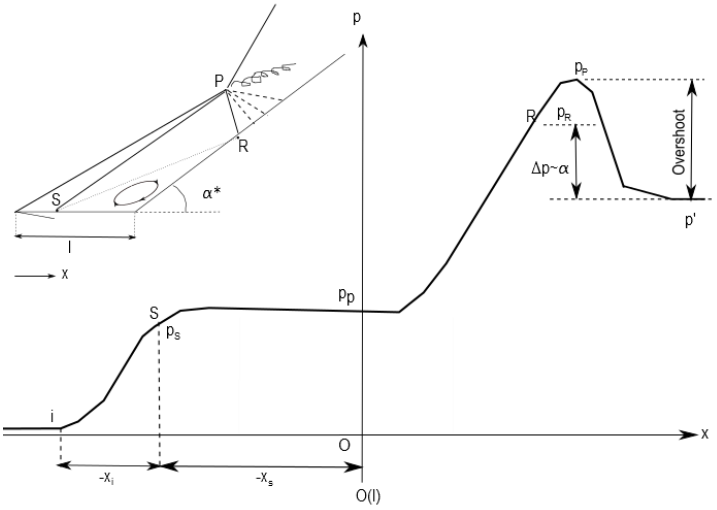

Figure 4: Schematic of pressure distribution in a hypersonic SBLI.

DOI: 10.13009/EUCASS2017-619

2.3 Secondary Vortices

In recent years, it has been shown that when separation is large, there may be no single recirculating eddy but that the separated region may consist of secondary or even tertiary eddies embedded within it. Discussion of such a feature in large separated flows has been presented by Smith [12], Smith and Khorrami [3], and Korolev et al. [4]. Dependence of these multiple eddies on wall temperature and Reynolds number has recently been investigated by Neiland et al. [1] and Shvedchenko [2] in hypersonic SBLI.

A measure of the extent of separation can be expressed in terms of the scaled angle α discussed in Rizzetta [13]. Studies by Smith and Khorrami [3], Korolev et al. [4], and Shvedchenko [2] show that a secondary eddy begins to appear when $4 \leq \alpha \leq 5$. A steady secondary eddy persists up to $\alpha \geq 6$. Beyond this, an instability sets in leading to further fragmentation into multiple eddies.

Possible factors leading to the occurrence of secondary eddies are, perturbation strength, Mach number M_∞, Reynolds number *Re*, and the wall temperature to stagnation temperature ratio S_w *(=* T_w/T_o*)*. Then, if Π is a parameter influencing the formation of eddies,

$$\prod = f(M_\infty, \mathrm{Re}, \alpha^*, S_w) \tag{1}$$

Based on the triple-deck theory, the perturbation strength α is expressed (see Rizzetta [13] ; Smith and Khorrami [3]; Korolev et al. [4]) as,

$$\alpha = \frac{\alpha^* \,\mathrm{Re}^{1/4}}{C^{1/4}\lambda^{1/2}\beta^{1/2}} \tag{2}$$

where α^* is typically a geometric angle in a compression corner or a corresponding semi-angle of a wedge generating a shock wave incident on a boundary layer on a flat plate provoking separation. *C* is Chapman-Rubesin constant, λ the Blasius shear, and $\beta = \sqrt{M_\infty^2 - 1}$. For hypersonic flows $\beta \approx M_\infty$. For a given Mach number,

$$\prod = f(\mathrm{Re}, \alpha, S_w) \tag{3}$$

The Reynolds number and wall temperature dependence can be combined in terms of alternate Reynolds number Re_w where,

$$\mathrm{Re}_w = \mathrm{Re}\left(\frac{\mu_\infty}{\mu_w}\right) \tag{4}$$

showing the dependence only on α and Re_w (Potter [14]). In what follows, we restrict ourselves to only an isothermal wall with one baseline temperature.

3. Results

3.1 Compression Corner

This is a much studied SBLI configuration both experimentally (for example, Holden [15]; Lewis et al. [16]; Délery et al. [17]; Mallinson et al. [18]) and numerically (Hung and Maccormack [19]; Rudy et al. [20]; Holden et al. 2003; Olejniczak and Candler [21]; Deepak et al. [22]). These studies present an exhaustive discussion and detailed analyses of both experimental as well as numerical simulations, which have shown agreement of varying degree with one another. None of these studies, however, mentions or discusses details of the internal structure of the separation bubble such as the existence or possibility of secondary vortices mentioned earlier in Section 2 although some of the studies involved large separations.

In the present study, we reconsidered the compression corner study of Mallinson et al. [18] and conducted a numerical investigation of a typical low enthalpy flow h_o = 2.83 *MJ/kg*, M_∞ = 9.1, $Re_\infty = 32.2 \times 10^5/m$, for two corner angles of 18º and 24º which yield moderate to large separated flows. For the flow conditions of the experiments the corresponding scaled angle α are 4.8 and 6.4, respectively. **Figs. 5(a)-(c)** show the results of nondimensional surface

DOI: 10.13009/EUCASS2017-619

pressure C_p, shear stress C_f, and heat flux C_h respectively for the 24º compression corner. The pressure curve illustrates all the major features of a large separated region as delineated in **Fig. 1**. Of particular note is the initial rise in pressure up to separation (*s*) followed by a long plateau region of near constant pressure and then a gradual rise up to reattachment (*r*). The recompression process continues rapidly until it reaches a peak identifying the neck region. The pressure then falls fairly rapidly till it reaches the final value *p'*. It is worth noting that just prior to the end of the plateau region and before the recompression process begins, there is a small dip in the pressure ($x \approx 0.08$). This indicates the presence of a secondary vortex in the vicinity of the corner (see Korolev et al. [4]). This is reflected in the positive shear stress within the main recirculation region (see **Fig. 5b**). The heat flux distribution is consistent with the pressure and shear stress curves. The insets in **Figs. 5(a)-(c)** show fluctuations in the pressures, shear stress, and heat flux in the corner region where the secondary eddies exist.

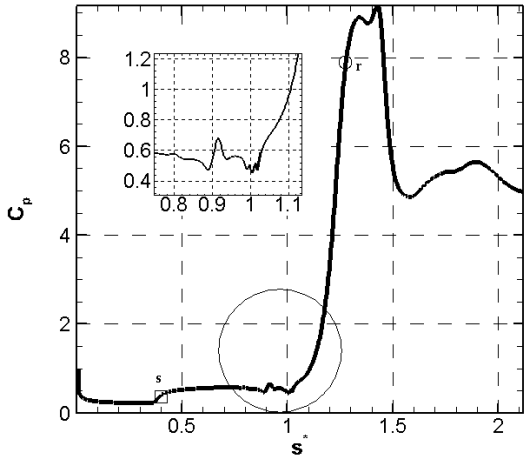

(a) Surface pressure.

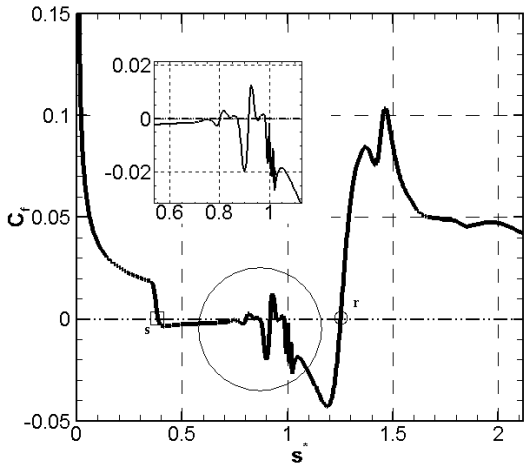

(b) Shear stress.

DOI: 10.13009/EUCASS2017-619

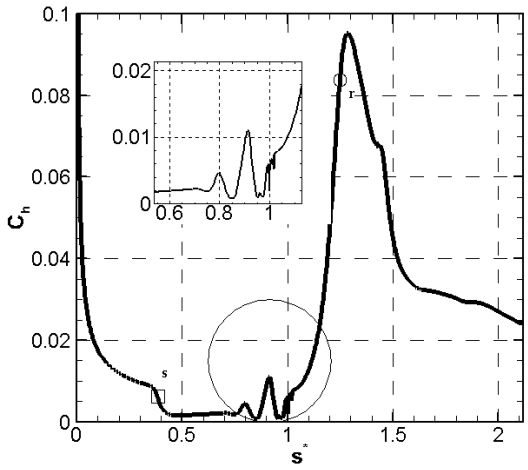

(c) Heat flux.

Figure 5: Compression corner separation (24º). Insets show the corner region.

Figs. 6(a) & **(b)** show contour plots of pressure and temperature on which streamlines are superposed in the separation bubble. A secondary vortex is clearly seen at the corner embedded within the main bubble. Further smaller eddies can also be seen upstream and downstream of the corner. Another feature to note is the shallow angles of separation and reattachment. As discussed earlier, when $6 \leq \alpha \leq 7$, flow instability sets in giving rise to fragmentation of eddies and it is possible the entire separation region becomes unsteady. It is worth noting that presence of these eddies is very difficult to verify experimentally in view of their scale and especially in short-duration facilities. Only indirect verification through shear stress measurements is a possibility but sometimes even this may not be feasible. To our knowledge, no direct experimental evidence of the presence of multiple vortices at large α exists at present.

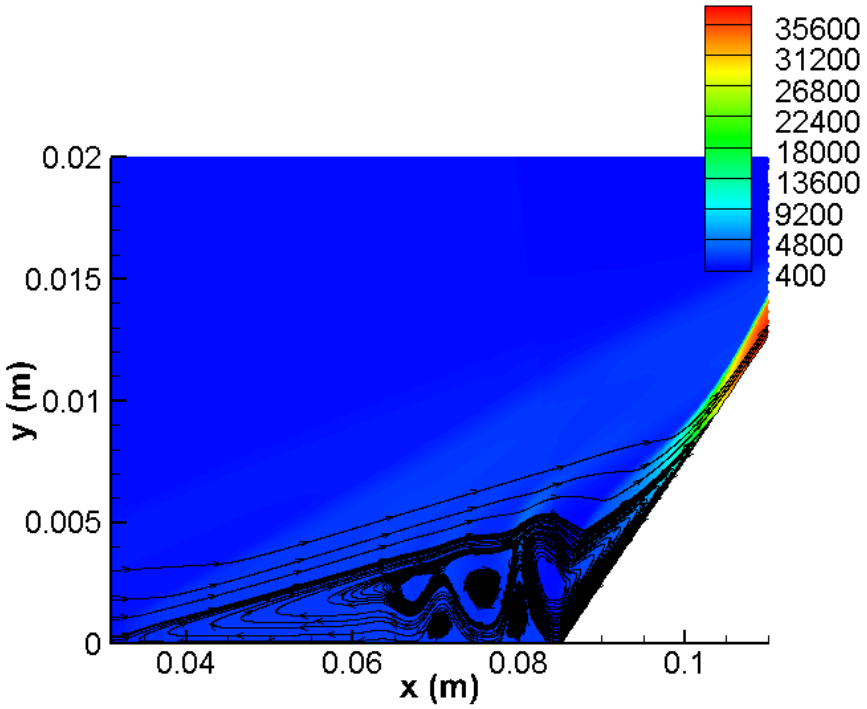

(a) Pressure (Pa).

DOI: 10.13009/EUCASS2017-619

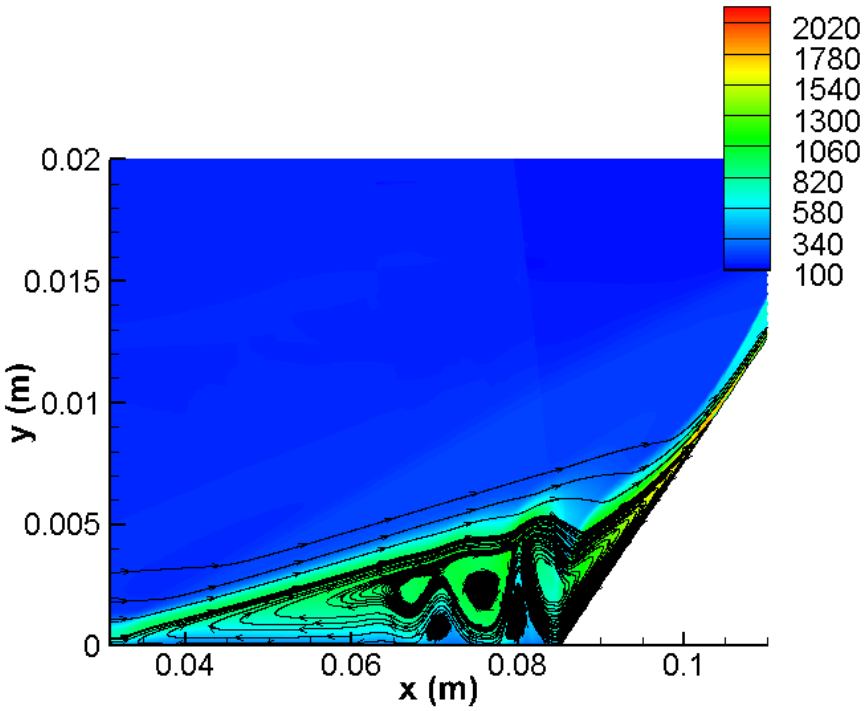

(b) Temperature (K).

Figure 6: Pressure and temperature contours of the 24° compression corner. Streamlines show fragmentation of separation region.

3.2 Leading Edge Separation

The leading edge separation configuration is a limiting case of a compression corner wherein the distance between the leading edge and separation point goes to zero (see Chapman et al. [8]; Khraibut et al. [23]). Although the configuration assumes no boundary layer growth before separation, in reality, there is a small boundary layer growth prior to separation. This is especially true in the case of hypersonic low Reynolds number flows such as those being considered in the present context. Because of the existence of a not well developed Blasius type boundary layer prior to separation, some of the standard assumptions made in the formulation and application of the triple-deck theory to such separations becomes questionable and suitable corrections need to be made (Khraibut et al. [23]).

Fig. 7 shows schematic of the leading edge separation with the main flow features. Here the corner angle B is such as to ensure separation at or very near the leading edge A. The configuration is equivalent to a compression corner of 55° exposed to a Mach number $M_\infty/cos(\alpha^*)$ where again M_∞ is the freestream Mach number and α^* is the compression corner angle. Ideally, after expansion at *A*, a thin shear layer, in which the velocity varies from zero to the local external stream value, springs from A and reattaches on the surface *BD* at *C*. A large recirculation region *ABC* is then formed bounded by the surface *ABC* and the shear layer *AC*. A weak shock precedes the strong expansion due to viscous effects at the leading edge. As can be seen, this is a large separated flow. The freestream conditions were h_o = 3.1 *MJ/kg*, M_∞ = 9.66, and $Re_\infty = 13.4 \times 10^5$.

DOI: 10.13009/EUCASS2017-619

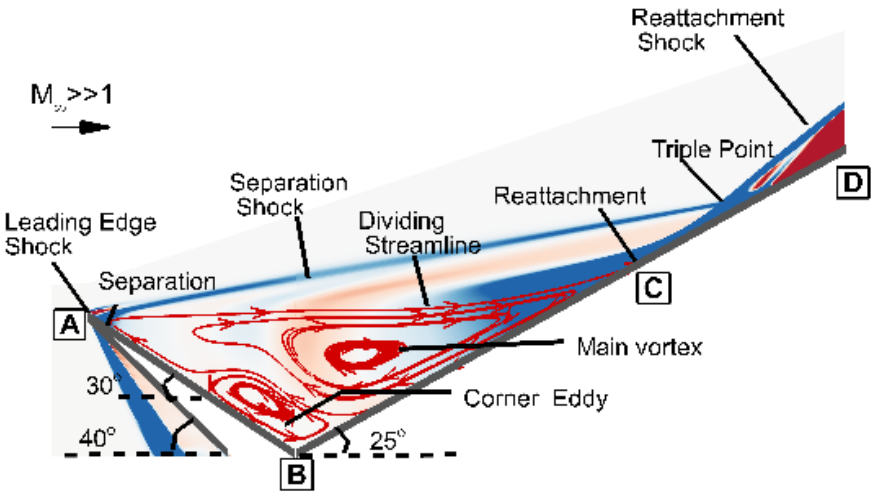

Figure 7: Schematic of the leading edge separation.

Figs. 8(a), **(b)**, and **(c)** show the nondimensional pressure, shear stress, and heat flux distributions for this flow. Looking at the pressure distribution, we can clearly delineate the various regions under the triple-deck framework. Although the boundary layer growth is small, we can still identify the interaction region $O(lRe^{-3/8})$ and separation point *s*, which is then followed by a long plateau of length $O(l)$, where l is a characteristic length, which is here taken as length of surface *AB*. Finally, the reattachment process which is largely inviscid as discussed earlier takes place over a distance $O(lRe^{-1/2})$ in which the pressure rises from the plateau value to the reattachment pressure at *r*. This can be further elucidated by examining the shear stress distribution curve in **Fig. 8(b)** where the beginning of reattachment can be taken from the point of negative shear stress peak just before reattachment to where the shear stress becomes positive and the shear stress jumps quite rapidly.

The inset in the shear stress distribution in **Fig. 8(b)** shows a positive double-loop structure on either side of the corner, which indicates the existence of a secondary/corner eddy embedded within the main vortex. The double-loop nature of this eddy is due to the corner discontinuity where the shear stress must go to zero at the vertex. **Fig. 9** shows the corresponding streamlines superposed on contours of temperature. Important features to be noted here are the secondary/corner eddy is asymmetrically disposed towards the expansion surface *AB*, while the main vortex is centred slightly towards the compression surface *BD*. The secondary eddy occupies almost half of the expansion surface length. This asymmetrical position of the secondary eddy is because the wall is colder than the outer recirculatory flow as seen from the temperature distribution within the recirculation region, the temperature increasing as the mixing layer is approached. The movement of the secondary eddy and the primary vortex away from the leading edge and towards the trailing edge as the wall temperature is increased has been discussed in detail in Khraibut et al. [23]). The analogy between vorticity and thermal energy distribution to first order in a recirculating flow has also been noted and discussed by Burggraf [24].

DOI: 10.13009/EUCASS2017-619

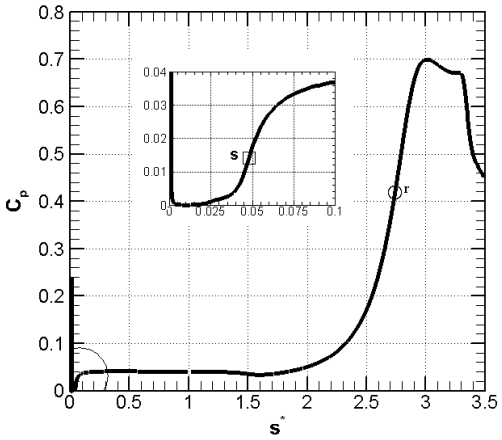

(a) Surface pressure;

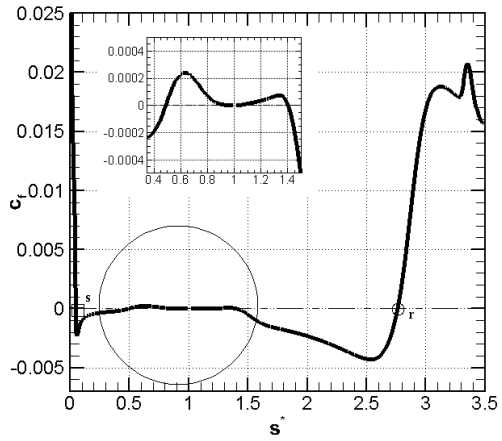

(b) Shear stress.

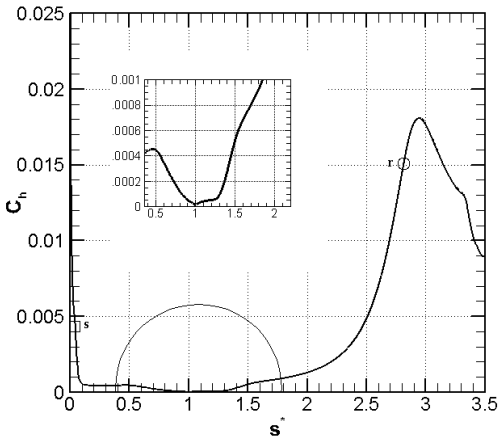

(c) Heat flux.

Figure 8: Leading edge separation with insets showing corner region.

DOI: 10.13009/EUCASS2017-619

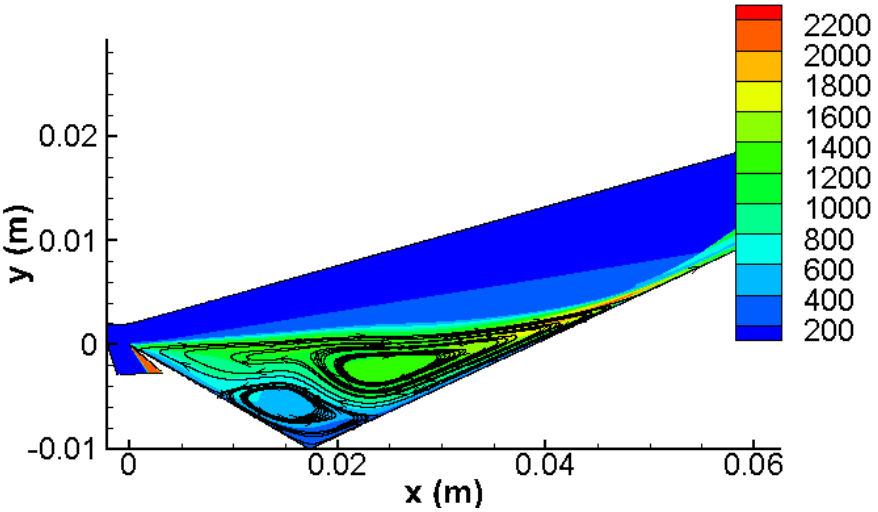

Figure 9: Temperature contours (K).

The existence and significance of an eddy at a corner in an incompressible flow was first discussed by Dean and Montagnon [25] and later rigorously analysed by Moffatt [26]. Moffatt showed that due to low local Reynolds numbers, a Stokes-like flow exists in the vicinity of the corner and gives rise to a sequence of eddies and provided the included corner angle is less than about 146º, the magnitude of these eddies diminishes rapidly in a geometric progression as the corner approaches. Moffatt also suggests that eventually only one or two eddies might exist at the corner. Thus, in a large separated flow, while the main recirculating region remains largely inviscid (Stewartson and Williams [9]), embedded within it are one or more secondary eddies which are generally of a size no more than 10% of the main vortex.

Appearance of a secondary vortex within the main recirculating region of hypersonic near wakes has been noted in the numerical simulations done by Grasso and Pettinelli [27] and Bashkin et al. [28]. Grasso and Pettinelli [27] attribute this feature to accumulation and spread of vorticity in the recirculating region, which in turn, is a strong function of the dividing streamline (DSL) Reynolds number Re_d $(=\rho_d u_d l_{dsl}/\mu_d)$, where ρ_d,u_d, μ_d, and l_{dsl}, are density, velocity, viscosity, and length of the dividing streamline, respectively. They suggest a range of Re_d wherein the vorticity in the recirculating region is dominated by either diffusion (Red $\leq$ 100) or convection ($Re_d \approx 300$). When $Re_d \geq 500$, a secondary vortex might appear due to an increase in the production of vorticity. These changes to vorticity field result from localized variations in the diffusion rate as a consequence of changes in temperature gradients occurring in the flow. In the present separated flow, the DSL Reynolds number Re_d is about 1500 so that secondary vortices can appear and that the vorticity is largely convection dominated. We also note from **Fig. 10** that the major part of the recirculating region is a near constant vorticity core bounded by shear and boundary layers.

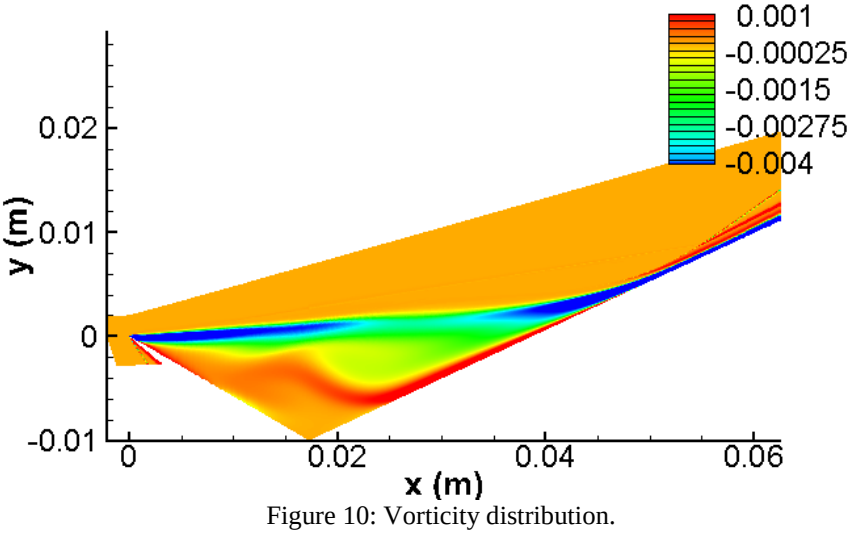

Figure 10: Vorticity distribution.

DOI: 10.13009/EUCASS2017-619

An interesting question still to be resolved is the distinction between a secondary eddy and a corner eddy in the Moffatt sense. From earlier studies (see Khraibut et al. [23]), it was revealed that development and movement of these secondary eddies is very much temperature dependent. For example, with very cold wall ($S_w = 0.05$), the secondary eddy was well upstream of the small corner eddy. However, when the wall temperature was increased ($S_w = 0.1$), the two eddies amalgamated with the single larger eddy moving downstream and lodged at the corner. In contrast, the compression corner data discussed earlier (**Fig. 5**) show the secondary vortices, one located just ahead and the other downstream of the corner, where $S_w = 0.125$. This movement of vortices downstream with increasing wall temperature has also been confirmed by Shvedchenko [2] for corner angles of 10^0 or more.

3.3 Incident Shock Separation

Most of laminar shock-induced separation analyses in terms of triple-deck theory have so far concerned mainly with compression corners and there seems very little attention paid to the incident shock-induced separation although this was one of the earliest examples of SBLI that was investigated (for example, Gadd et al. [29]; Hakkinen et al. [30]; Lees and Reeves [31]). It is therefore worth examining this configuration in the present context. In a free interaction, the behaviour of the boundary layer is the same whether separation is provoked by an incident shock, a compression corner, or a step. It follows, therefore, that provided the total pressure rise is the same and the flow has undergone the same amount of flow deflection, the effects due to interaction of an incident shock and a compression corner are equivalent. Thus an incident shock deflection of α^* from a wedge is equivalent to a compression corner deflection angle of $2\alpha^*$ at the same Mach and Reynolds number.

Detailed numerical and experimental investigations of the incident shock/laminar boundary layer interaction in supersonic flow under adiabatic wall condition have been made in recent years by Degrez et al. [32] and Katzer [33]. In these studies, time accurate two-dimensional compressible Navier-Stokes equations were solved and compared with experimental data of Degrez et al. [32]. The Mach and Reynolds number range covered was $1.4 \leq M_\infty \leq 3.4$ and $1 \times 10^5 \leq Re \leq 6 \times 10^5$, respectively. The Reynolds number was based on freestream conditions and distance from the leading edge of the plate to the shock impingement location. Comparison showed good agreement. Katzer [33], in particular, compared his numerical data with triple-deck theory and found that, in general, the triple-deck theory seemed to over-predict the Navier-Stokes data and the discrepancy was found to increase with increase in Mach number and decrease in Reynolds number. There do not appear to be comparable investigations in hypersonic flows with this configuration. Herein, we present some numerical Navier-Stokes solutions of hypersonic incident shock/laminar boundary layer interaction and interpret them in terms of triple-deck theory. The parameters in the study were freestream mach number $M_\infty = 5.85$; Reynolds number $Re_{xc} = 13.3 \times 10^5$; $S_w = 0.5$. A shock wave from a wedge of semi-angle 10^o was incident on a laminar boundary layer developed on a sharp flat plate of length 230 mm. The point of incidence of the shock wave x_c was 186 mm from the leading edge of the plate. **Fig. 11** shows a schematic of the configuration.

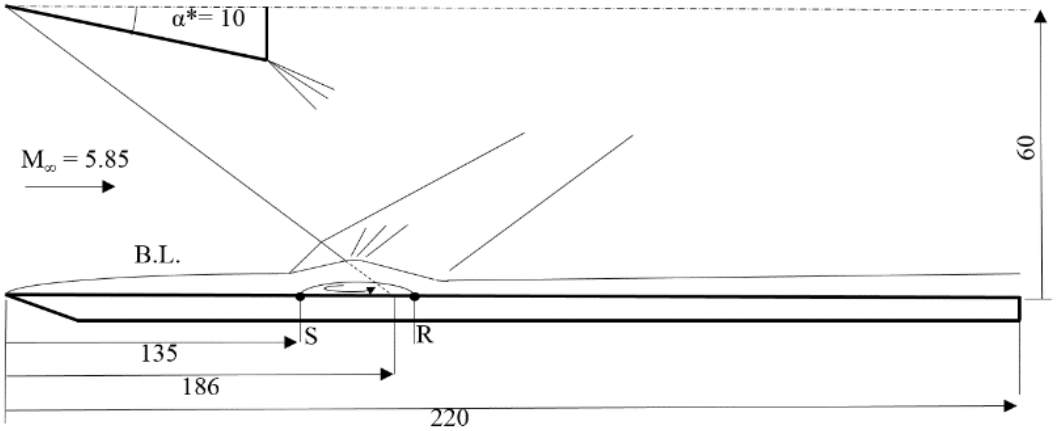

Figure 11: Schematic of incident shock separation.

Figs. 12(a)-(c) show pressure, shear stress, and heat flux in terms of C_p, C_f, and Stanton number *St*. All the characteristics of a typically large separated region as discussed in relation to **Fig. 1** are seen here also. Both the pressure and the shear stress clearly indicate a secondary eddy just ahead of the shock impingement location. The pressure is characterised by a small dip and the shear stress goes positive at $x/x_o \approx -0.14$ and after a small double peak goes negative again at $x/x_o \approx -0.086$. The heat flux increases to a peak at $x/x_o \approx 0.14$ and then goes through a minimum

DOI: 10.13009/EUCASS2017-619

at $x/x_o \approx$ -0.086 before rising again. The plateau region which extends between -0.516 $\leq x/x_o \leq$ -0.14 is *O(l)*, which indeed, is in accordance with the asymptotic theory.

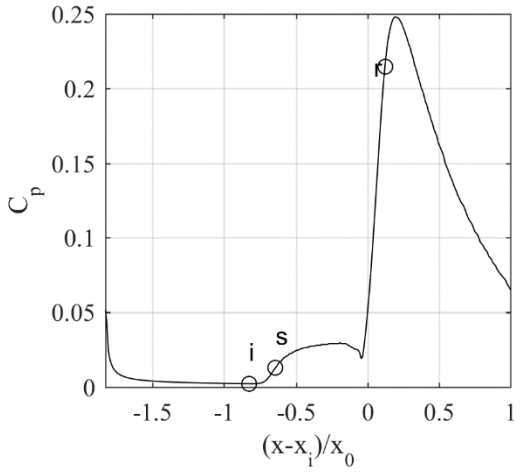

(a) Surface pressure.

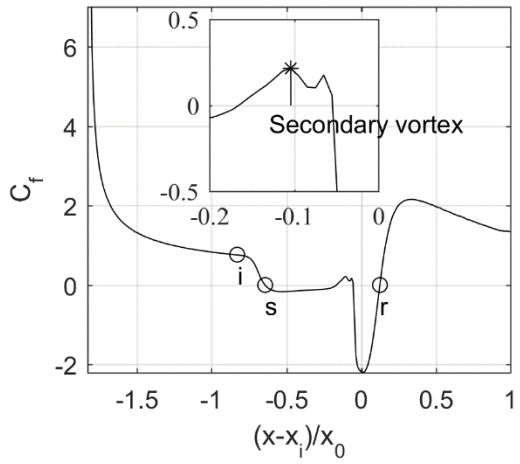

(b) Shear Stress.

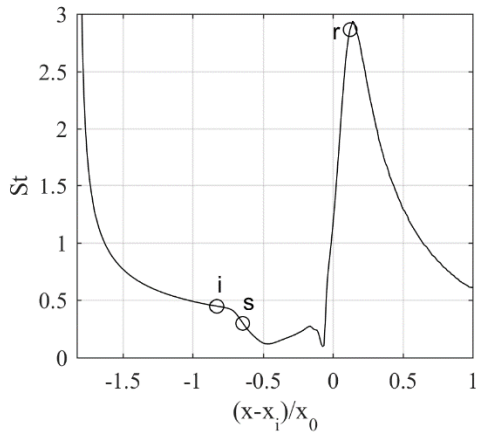

(c) Heat flux.

Figure 12: Incident shock separation.

DOI: 10.13009/EUCASS2017-619

3.4 Structure of the Separation Bubble

All the configurations considered here, are characterised by a large separation bubble where $\alpha \geq 3.5$ and the length is *O(l)*. Burggraf [5] has shown that the bubble length scales as $\alpha^{3/2}$. **Fig. 13** shows the bubble length X_B, the distance between separation and reattachment plotted against $\alpha^{3/2}$, which shows a linear relation. The zero intercept gives $\alpha \approx 3$, which is when the plateau region has fully developed, a characteristic of large separation (see Burggraf [5]). More interestingly, the figure illustrates the generality of this relationship, which appears to be independent of the mode of generating large separations, a basic assumption of Neiland's asymptotic theory of large separated flows. It should be noted that, so far, most of the large separation analyses within the framework of triple-deck theory have been in terms of the compression corner configuration (Burggraf [5]; Rizzetta et al. [7]; Korolev et al. [4]; Neiland et al. [1]; and Shvedchenko [2]). Herein, we have shown it to be true in the case not only of the compression corner but also incident shock, and the leading edge separation, which can be considered an extreme example of separation geometry. The range also extends from supersonic (Chapman et al. [8]; Degrez et al. [32]; Katzer [33]; Korolev et al. [4]) to hypersonic SBLIs.

A second characteristic of large separation is the higher (in magnitude) negative shear stress minimum just before reattachment. This sharp minimum in shear stress was first discussed as a possible 'reverse flow singularity' by Smith and Khorrami [3]. Later, it was argued by Korolev et al. [4] that there need be no singularity and that the reattachment is smooth after passing through this sharp minimum. We would also point out here that in our computations too of compression corner, leading edge separation (Khraibut et al. [23]), and incident shock, the reattachment reached smoothly after passing through a sharp negative minimum. Based on Neiland's asymptotic theory, Korolev et al. [4] show that $|\tau_w|_{min} \sim \alpha$. **Fig. 13** shows $|\tau_w|_{min}$ plotted against α for the three configurations considered here. We note that the variation of $|\tau_w|_{min}$ appears linear up to about $\alpha \approx 6$ but beyond that the shear stress rise is quite sharp as the largest separation case of compression corner with $\alpha^* = 24^0$ ($\alpha = 6.42$) is reached. It is, therefore, possible that the validity of the linear relationship between $|\tau_w|_{min}$ and α in a two-dimensional separation does not extend beyond $\alpha \geq 6$. It can therefore be argued that even in a larger separated region, there is a stable flow regime beyond which rapid fragmentation of the flow in the recirculation region occurs in the form of instabilities in secondary vortices giving rise to further small scale eddies.

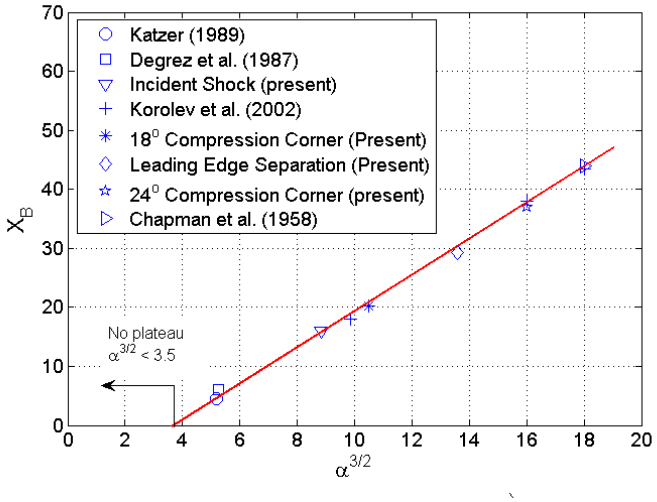

Figure 13: Length of the separation bubble as a function of the scaled angle.

Fig. 14 is consistent with the observations of Shvedchenko [2] that stable secondary eddies at $4 \leq \alpha \leq 5$ give rise to instabilities beyond $\alpha \approx 6$. This is in line with the suggestion Smith and Khorrami [3] that such instabilities can arise due to non-zero normal pressure gradients resulting in changes to the structure in the reverse flow region. A point also made by Neiland et al. [1]. While all these earlier studies were confined to the compression corner configuration, it is shown here that the classification is valid irrespective of the mode of provoking the separation.

DOI: 10.13009/EUCASS2017-619

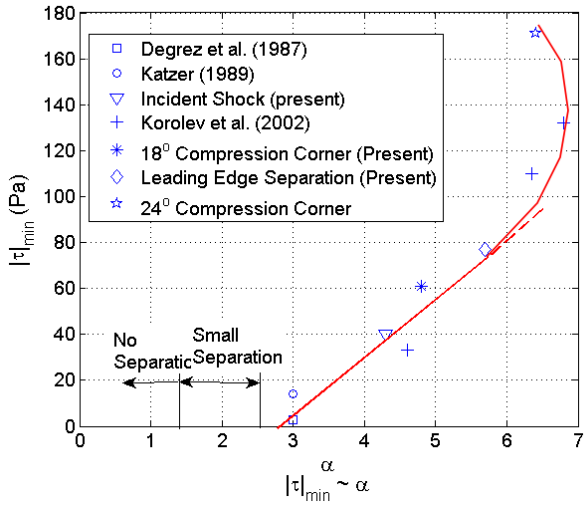

Figure 14: Variation of second minimum in the bubble as a function of the scaled angle.

It is worth pointing out here that although the actual length of the separation region (that is, the distance between separation and reattachment points) is slightly different from the length of the pressure plateau, they have been used synonymously in literature (for example, Korolev et al. [4]). As defined by Burggraf [5], the plateau length $l_p \sim \alpha^{3/2}$ while Korolev et al. [4] assume $l_B \sim \alpha^{3/2}$, where l_B is the bubble length. In actual fact, the bubble length comprises the plateau length and two small regions of length $O(lRe^{-1/2})$ after separation before plateau begins and another length $O(lRe^{-1/2})$ just after the end of plateau and before reattachment. In the present instance, we take bubble length to vary as $\alpha^{3/2}$.

Another possible reason for the evolution of multiple vortices in a stable separation bubble is the change in the pressure field occurring as a consequence of superposition of longitudinal disturbances generated within the bubble. As suggested by Theofilis [34], these longitudinal disturbances induce degeneracy in the shear stress distribution, triggering thereby multiple structures in the bubble. Further, if these disturbances develop sufficient amplitude (by increasing α), three-dimensionality in the bubble structure will develop leading to both streamwise and spanwise instabilities. Theofilis [34] have anlaysed these instabilities in terms of linear stability theory. Defining the perturbed flow field as $Q(x,y,z,t)$ in terms of two-dimensional field on which is imposed a three-dimensional disturbance, then

$$Q(x,y,z,t) = Q_b(x,y) + \varepsilon Q_p(x,y)\exp i(\beta z - \Omega t) + c.c. + \ldots \quad (5)$$

where Q_b is a basic two-dimensional flow and Q_p is a superposed disturbance. ε (<< 1) defines the magnitude of the disturbance assumed small in order that linearization is valid. β is a real wave number and Ω, the complex eigen value that contains frequency and temporal growth rate of the disturbance. Using this theory, Theofilis [34] show that instabilities in the separation bubble are a function of growth rate of disturbances propagating through the bubble. It must be pointed out that the above theory is basically built around an incompressible flow and its validity in supersonic/hypersonic boundary layers is not known although for low velocities that usually prevail in a separation bubble they may be approximately valid.

Another aspect of these secondary vortices and instabilities is their apparent absence in axisymmetric flows. Computations done by Gittler and Kluwick [10] on a flared cylinder in supersonic flow, show no secondary eddy even for α as high as 9. This is more than a factor of two compared to a two-dimensional compression ramp. Their calculations show that the characteristic double-trough in negative skin friction and plateau of a large separated region do not begin till $\alpha \geq 5$. The steep increase in negative skin friction prior to reattachment also begins at $\alpha \approx 5$. These results are consistent with the fact that separation and reattachment phenomena are milder in axisymmetric flows in comparison with their two-dimensional counterpart. This is also obvious from inspection of the stability equation of Theofilis [34] mentioned above. It is also worth mentioning the absence of secondary eddy in well-known double-cone simulations (for example, Nompelis et al. [35]) in contrast to double-wedge solutions Olejniczak and Candler [21]).

DOI: 10.13009/EUCASS2017-619

4. Summary and Conclusions

The analysis of large separations in supersonic and hypersonic SBLIs is presented within the framework of asymptotic theory of Neiland [36] and Stewartson and Williams [9]. It is seen that the separation bubble is made of three distinct regions – an initial free-interaction region up to separation of $O(lRe^{-3/8})$, a long plateau region of $O(l)$, and a nearly inviscid reattachment region of $O(lRe^{-1/2})$. It was found that the size of the separated region was strongly dependent on the scaled angle α (representing the perturbation strength) being proportional to $\alpha^{3/2}$. While previous investigations addressed the problem only in terms of separation induced by a compression corner configuration, here for the first time, it is shown that the phenomenon is more general by considering the other often used configuration of an incident shock-induced separation of a boundary layer on a flat plate. We have also shown it to be true in the case of a leading edge separation, which is a limiting case of the compression corner.

The study has further shown that the magnitude of the (negative) skin friction before reattachment varies linearly irrespective of the mode of instigating separation up to $\alpha \approx 6$ beyond which further fragmentation of vortices occurs triggering instability within the separation bubble, consistent with earlier compression corner investigations of Neiland et al. [1] and Shvedchenko [2]. The present study, while confined to a single wall temperature, effects of wall temperature will be dealt with in another paper.

Acknowledgements

This work was supported by the Australian Research Council through the Grant DP-40100842 to which the authors are grateful. We would also acknowledge the National Facility System (NCI) for providing computer resources.

References

[1] Neiland, V.Y., L.A. Sokolov, and V.V. Shvedchenko, Temperature factor effect on separated flow features in supersonic gas flow, in *BAIL 2008-Boundary and Interior Layers*. 2009, Springer. p. 39-54.

[2] Shvedchenko, V.V., About the secondary separation at supersonic flow over a compression ramp. *TsAGI science journal,* 2009. **40**(5).

[3] Smith, F.T. and A.F. Khorrami, The interactive breakdown in supersonic ramp flow. *Journal of Fluid Mechanics,* 1991. **224**: p. 197-215.

[4] Korolev, G.L., J.B. Gajjar, and A.I. Ruban, Once again on the supersonic flow separation near a corner. *Journal of Fluid Mechanics,* 2002. **463**: p. 173-199.

[5] Burggraf, O.R., Asymptotic theory of separation and reattachment of a laminar boundary layer on a compression ramp, in *AGARD-CP-168*. 1975.

[6] Daniels, P.G., Laminar boundary-layer reattachment in supersonic flow. *Journal of Fluid Mechanics,* 1979. **90**(02): p. 289-303.

[7] Rizzetta, D.P., O.R. Burggraf, and R. Jenson, Triple-deck solutions for viscous supersonic and hypersonic flow past corners. *Journal of Fluid Mechanics,* 1978. **89**(03): p. 535-552.

[8] Chapman, D.R., D.M. Kuehn, and H.K. Larson, Investigation of separated flows in supersonic and subsonic streams with emphasis on the effect of transition. *NACA Technical Report 1356,* 1958.

[9] Stewartson, K. and P.G. Williams, On self-induced separation II. *Mathematika,* 1973. **20**(01): p. 98-108.

[10] Gittler, P. and A. Kluwick, Triple-deck solutions for supersonic flows past flared cylinders. *Journal of Fluid Mechanics,* 1987. **179**: p. 469-487.

[11] Edney, B.E., Effects of shock impingement on the heat transfer around blunt bodies. *AIAA Journal,* 1968. **6**(1): p. 15-21.

[12] Smith, F.T., A reversed flow dingularity in interacting boundary layers. *Proceedings of the Royal Society of London A: Mathematical, Physical and Engineering Sciences,* 1988.

[13] Rizzetta, D.P., Asymptotic solution for two-dimensional viscous supersonic and hypersonic flows past compression and expansion corners. *Ph.D. Thesis*, 1976.

[14] Potter, J.L. The transitional rarefied flow regime. in *5th International Symposium on Rarefied Gas Dynamics*. 1966. University of Oxford: Academic press.

[15] Holden, M.S., Experimental studies of separated flows at hypersonic speeds. II-Two-dimensional wedge separated flow studies. *AIAA Journal,* 1966. **4**(5): p. 790-799.

[16] Lewis, J.E., T. Kubota, and L. Lees, Experimental investigation of supersonic laminar, two-dimensional boundary-layer separation in a compression corner with and without cooling. *AIAA Journal,* 1968. **6**(1): p. 7-14.

DOI: 10.13009/EUCASS2017-619

[17] Délery, J., J.G. Marvin, and E. Reshotko, Shock-wave boundary layer interactions. *AGARDograph-AG-280*, 1986.
[18] Mallinson, S.G., S.L. Gai, and N.R. Mudford, High-enthalpy, hypersonic compression corner flow. *AIAA Journal,* 1996. **34**(6): p. 1130-1137.
[19] Hung, C.M. and R.W. MacCormack, Numerical solutions of supersonic and hypersonic laminar compression corner flows. *AIAA Journal,* 1976. **14**(4): p. 475-481.
[20] Rudy, D., J. Thomas, A. Kumar, P. Gnoff, and S. Chakravarthy. A validation study of four Navier-Stokes codes for high-speed flows. in *20th Fluid Dynamics, Plasma Dynamics and Lasers Conference*. 1989.
[21] Olejniczak, J. and G. Candler. Computation of hypersonic shock interaction flow fields. in *7th AIAA/ASME Joint Thermophysics and Heat Transfer Conference*. 1998.
[22] Deepak, N.R., S.L. Gai, and A.J. Neely, A computational investigation of laminar shock/wave boundary layer interactions. *The Aeronautical Journal,* 2013. **117**(1187): p. 27-56.
[23] Khraibut, A., S.L. Gai, L.M. Brown, and A.J. Neely, Laminar hypersonic leading edge separation--a numerical study. *Journal of Fluid Mechanics,* 2017. **821**: p. 624-646.
[24] Burggraf, O.R., Analytical and numerical studies of the structure of steady separated flows. *Journal of Fluid Mechanics,* 1966. **24**(01): p. 113-151.
[25] Dean, W.R. and P.E. Montagnon, On the steady motion of viscous liquid in a corner. 1949. **45**(03): p. 389-394.
[26] Moffatt, H.K., Viscous and resistive eddies near a sharp corner. *Journal of Fluid Mechanics,* 1964. **18**(01): p. 1-18.
[27] Grasso, F. and C. Pettinelli, Analysis of laminar near-wake hypersonic flows. *Journal of Spacecraft and Rockets,* 1995. **32**(6): p. 970-980.
[28] Bashkin, V.A., I.V. Egorov, M.V. Egorova, and D.V. Ivanov, Supersonic laminar-turbulent gas flow past a circular cylinder. *Fluid Dynamics,* 2000. **35**(5): p. 652-662.
[29] Gadd, G.E., D.W. Holder, and J.D. Regan. An experimental investigation of the interaction between shock waves and boundary layers. in *Proceedings of the Royal Society of London A: Mathematical, Physical and Engineering Sciences*. 1954.
[30] Hakkinen, R.J., I. Greber, L. Trilling, and S.S. Abarbanel, The interaction of an oblique shock wave with a laminar boundary layer. *NASA Memo 2-18-59W,* 1959.
[31] Lees, L. and B.L. Reeves, Theory of laminar near wake of blunt bodies in hypersonic flow. *AIAA Journal,* 1965. **3**(11): p. 2061-2074.
[32] Degrez, G., C.H. Boccadoro, and J.F. Wendt, The interaction of an oblique shock wave with a laminar boundary layer revisited. An experimental and numerical study. *Journal of Fluid Mechanics,* 1987. **177**: p. 247-263.
[33] Katzer, E., On the lengthscales of laminar shock/boundary-layer interaction. *Journal of Fluid Mechanics,* 1989. **206**: p. 477-496.
[34] Theofilis, V., On steady-state flow solutions and their nonparallel global linear instability. *Advances in turbulence VIII,* 2000: p. 35-38.
[35] Nompelis, I., G.V. Candler, and M.S. Holden, Effect of vibrational nonequilibrium on hypersonic double-cone experiments. *AIAA Journal,* 2003. **41**(11): p. 2162-2169.
[36] Neiland, V.Y., Asymptotic theory of plane steady supersonic flows with separation zones. *Fluid Dynamics,* 1970. **5**(3): p. 372-381.